

## Cylinder Test Characterization of an Ammonium Nitrate and Aluminum Powder Explosive

David L. Robbins<sup>†</sup>, Eric K. Anderson<sup>†</sup>, Mark U. Anderson<sup>‡</sup>, Scott I. Jackson<sup>†</sup> and Mark Short<sup>†</sup>

<sup>†</sup>Los Alamos National Laboratory, Los Alamos, NM, 87545

<sup>‡</sup>Sandia National Laboratories, Albuquerque, NM 87123

**Abstract.** While ammonium nitrate is itself detonable, its sensitivity and performance, when combined with aluminum powder, are substantially increased. In the present work, the results of a series of cylinder tests to characterize the performance of this explosive are reported. In the test series, the cylinder size is varied to determine the effect of cylinder diameter on performance. Explosive performance is characterized in terms of the detonation energy and velocity. Results will allow determination of the explosive product equation of state and extent of aluminum reaction in the detonation reaction zone.

### Introduction

Ammonium nitrate (AN) mixed with aluminum powder is a non-ideal explosive (explosive that releases energy after the detonation sonic surface) that exhibits a wide range of behaviors depending on the particle size, morphology, and ratio of the components. While pure AN is not generally used as an explosive, it will detonate and experiments have shown that manila paper tubes packed with AN will detonate down to a critical diameter of 10-15 cm<sup>1</sup>. Detonation velocities of 1.1 mm/ $\mu$ s at the critical diameter, and up to 2.8 mm/ $\mu$ s for 46 cm charges, have been reported for AN packed in manila paper tubes to a density of 1 g/cc<sup>1</sup>. The addition of other explosives such as TNT, or fuels such as aluminum or organic materials can increase the sensitivity of AN<sup>2</sup>. Aluminum is considered the most effective sensitizer, reducing the critical diameter by an or-

der of magnitude<sup>2, 3, 4</sup>, yet the role it plays in the detonation reaction zone is not fully understood.

A significant effort to understand the combustion of aluminum was made in the 1960's and 1970's. Glassman<sup>5</sup> realized that metal combustion is analogous to droplet combustion, and that ignition and combustion behavior would depend on the melting and boiling points of the metal and oxide, and that metal particles with an oxide shell would not ignite until the melting point of the oxide was reached. He also observed that the rate of aluminum combustion in air is controlled by diffusion of the fuel and oxidizer. A simple hydrocarbon droplet combustion model, however, cannot be readily adapted to aluminum combustion due to the condensation of Al<sub>2</sub>O<sub>3</sub>, which contributes significantly to the heat release as well as potentially interfering with the combustion of the remaining aluminum<sup>6</sup>. Aluminum particles of several micron diameter or smaller suspended in air will also detonate<sup>7</sup>. Experimental observations have shown that the deflagration-to-detonation transition (DDT)

distance and detonation sensitivity are dependent on initial pressure. These observations suggest gas-phase kinetics, in addition to diffusion, are important in determining the reaction rate.

Mixtures of AN and aluminum powder have been referred to with several names, including ammonal and Tannerite (a brand name). Here we will refer to explosive mixtures of AN and aluminum powder as ammonals. Maranda<sup>4</sup> reported results of a study to investigate the influence of particle size of the aluminum and ammonium nitrate as well as oxide content of the aluminum on the detonation performance of ammonal. The results of the study showed that detonation velocity and critical diameter varied significantly depending on these parameters, which is not unusual for a non-ideal explosive. For example, when confined in a 36-mm-ID, 3-mm-thick steel tube, ammonal detonation velocity varied from approximately 1.2 mm/ $\mu$ s for 5-10% flaked aluminum with 30.9%  $\text{Al}_2\text{O}_3$  content and 1.2-2.0 mm granulated ammonium nitrate, to 3.67 mm/ $\mu$ s for granulated aluminum with a mean particle size of 59  $\mu$ m and 7.5%  $\text{Al}_2\text{O}_3$  blended with 0.06 to 0.3 mm diameter ground ammonium nitrate. Failure diameters were also dependent on the particle size, morphology, and oxide content, and ranged from 10 to 20 mm for 10/90 blends of aluminum powder/AN. These results underscore the need to carefully control particle characteristics in ammonal performance tests.

Other studies<sup>8, 2, 9, 3, 10</sup> have reported similar detonation velocities and failure diameters to those of Maranda, with critical diameter and detonation velocity dependent on particle size and morphology. Cylinder tests have been reported by Buczkowski and Zygmunt<sup>11</sup>, as well as Souers et al.<sup>12</sup>. Results showed detonation velocities ranging from 2.6 to 3.7 mm/ $\mu$ s.

It has previously been assumed that aluminum particles act as an inert in the detonation reaction zone of ammonal, combusting primarily in the post-reaction zone expansion of detonation products<sup>13</sup>. Here, we intend to investigate the role of aluminum in ammonal detonation in cylinder tests, where the explosive is confined in a precision-machined, oxygen-free high-conductivity (OFHC), 99.99% pure copper cylinder. The test allows observation of the expansion of the cylinder, which is af-

ected by the time history of the explosive-product energy-release. Analysis of the test can determine the kinetic energy of the cylinder wall as a function of time, until breakage of the cylinder occurs.

Additional insight into the rate of the aluminum reaction can be gained as the cylinder is scaled up in size. Non-ideal explosives, including ammonals, tend to exhibit increased energy output as the diameter of the charge is increased. In cylinder tests, this results in increasing cylinder-wall velocities with increasing cylinder-test diameter. This phenomenon is related to the well-known diameter effect, which refers to the increase in detonation velocity as the diameter of an explosive charge is increased. While the diameter effect on detonation velocity is observed in ideal and non-ideal explosives, the effect of diameter on wall velocity in a cylinder test depends on the promptness of reaction following the lead shock in the detonation. An ideal explosive that reacts quickly before the sonic surface would exhibit nearly identical scaled wall-velocity profiles across a range of cylinder-test diameters, whereas a non-ideal explosive exhibiting slower reactions tends to produce increased wall velocities as the diameter is increased. This effect can be attributed to the higher post-sonic-surface temperatures, which enable higher late reaction rates. By enabling the measurement of energy release at multiple charge diameters, scaled cylinder-tests provide a means to determine the "idealness" of an explosive.

## Experimental Setup

The aluminum powder used for this study is 99.8% pure, with a 10% mass fraction diameter (D10) of 2.05  $\mu$ m, D50 of 4.53  $\mu$ m, and D90 of 10.59  $\mu$ m. The ammonium nitrate prill was 98% pure and ground in a grain mill to a D50 of 850  $\mu$ m with a very narrow span (D90 - D10). The materials were combined dry to achieve a mass ratio of 9:1 ammonium nitrate to aluminum. Mixing was conducted by tumbling to assure a uniform mixture, and the copper cylinders were filled, hand tapping every third of the way to settle the material. Figure 1 shows a cylinder test assembly, and Table 1 lists the ammonal mass and density for each test.

Tests were conducted in copper cylinders scaled to two and three times the standard dimensions<sup>14</sup>;

the first test was conducted in a cylinder 2 in. inner diameter (ID), 2.4 in. outer diameter (OD), and 24 in. long. The dimensions of the cylinder in the second test were 3 in. ID, 3.6 in. OD, and 36 in. long. Tolerances were held to within 0.001 in. Both tubes were annealed for ductility; the smaller tube measured 25 on a Rockwell hardness F scale, while the large tube measured 35. These hardness values indicate the near-maximum ductility required for maximum expansion before rupture.

## Results

### Detonation Velocity

Each cylinder was detonated with eleven evenly spaced ionization wires to measure phase velocity,  $D_0$ , and results are reported in Table 1. These results, when combined with previous metal-confined tests of 90% ammonium nitrate, 10% aluminum powder, produce the diameter-effect curve of Fig. 2. It should be noted that the previous results reported in this figure were conducted with either 5, 20, or 95  $\mu\text{m}$  aluminum particle diameter and 60  $\mu\text{m}$  AN particles, but despite varying particle sizes, the current results agree well with the diameter-effect curve fit to the previous results, showing that cylinder diameter has a more significant effect on  $D_0$  than aluminum or ammonium nitrate particle size, at least within the range of sizes tested.

Table 1. Ammonal test results. Standard error associated with the linear fit to ionization wire data is reported following the  $\pm$  symbol.

Tube ID (mm)	Ammonal Mass (g)	Fill Density ( $\text{g}/\text{mm}^3$ )	$D_0$ (mm/ $\mu\text{s}$ )
2.000	1162.7	0.968	3.516 $\pm$ 0.020
3.000	3894.2	0.953	3.824 $\pm$ 0.009

### Wall Velocity Measurements

For each cylinder test, PDV probes were located at the positions listed in Table 2 and Table 3. Measurements  $z$  and  $r$  are as defined in Fig. 3. Each

Table 2. PDV probe locations, 2 in. cylinder test.

Probe #	Distance $z$ (mm)	Distance $r$ (mm)
1	94	144
2	94	144
3	196	144
4	196	144
5	296	144
6	296	144
7	387	131
8	502	131

Table 3. PDV probe locations, 3 in. cylinder test.

Probe #	Distance $z$ (mm)	Distance $r$ (mm)
1	151	151
2	151	165
3	304	144
4	304	146
5	456	166
6	456	163
7	608	162
8	761	146

probe was aligned normal to the tube surface. To ensure sufficient light collection during tube expansion, which causes tube wall angle relative to the probe to change, the tube surface was prepared in a manner that would scatter the light primarily along the tube axis ( $z$ -direction).

PDV velocities measured for the 2 in. cylinder are shown in Fig. 4. As the figure shows, good signals were obtained for all eight probes and the velocity profiles were consistent (each of the last three profiles show over lapping data from two probes). The time indicated in the figure is relative to the detonator trigger signal. In Fig. 5, velocities from each probe have been shifted to have the same jump-off times. Apart from probe 8, nearest to the booster end of the cylinder, the wall histories overlay well.

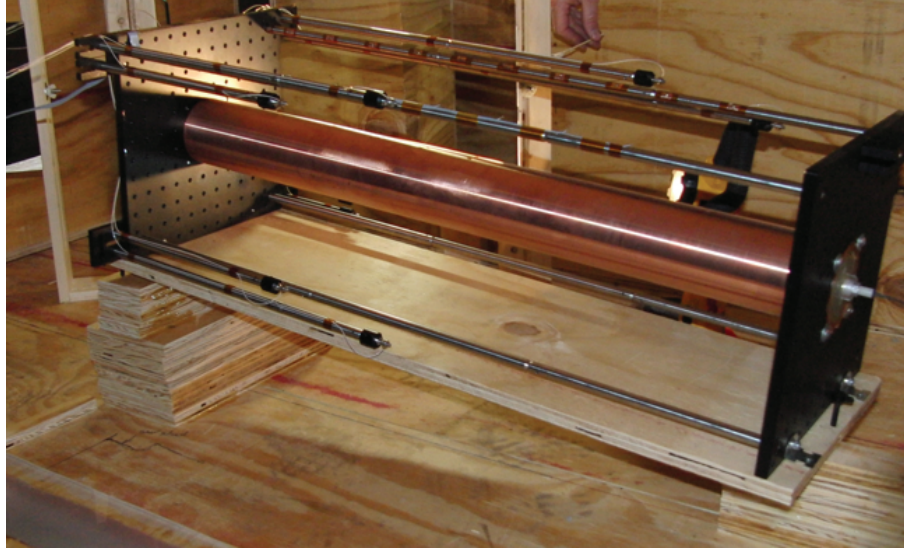


Fig. 1. Photograph of an ammonal cylinder test assembly.

Probe 8 exhibits the lowest velocities near the end of the measurement. Consistent velocity profiles produced by the rest of the probes indicate that the detonation in the 2-in. cylinder has relaxed to a quasi-steady state. Figure 6 shows position vs. time results computed from the velocity profiles. Again, good consistency between probes is apparent.

PDV velocities measured for the 3 in. cylinder are shown in Fig. 7. As the figure shows, good signals were obtained for six probes and the velocity profiles appear to demonstrate faster wall acceleration and higher peak velocities as probe distance from the booster end of the cylinder increased. The profiles diverge for the two probes with approximately  $125 \mu\text{s}$  jump-off time and also for the probes with  $158 \mu\text{s}$  jump-off time. These differences could be due either to the bore of the cylinder being off-axis from the outer surface, or setting of the ammonal before the shot was fired. In Fig. 8, velocities from each probe have been shifted to have the same jump off time. Unlike the 2-in. cylinder, the wall velocity history is continually modified as the detonation moves down the cylinder. Specifically, the wall accelerates more rapidly and attains progressively higher velocities. This indicates that, over time, additional energy is being generated in the conversion of reactants into equilibrium products. We con-

jecture that the higher post-sonic surface temperatures in the 3-in. cylinder allow late time energy release associated with the slow burning of aluminum, the effects of which become more pronounced as the detonation moves down the cylinder. Figure 9 shows position vs. time results computed from the velocity profiles.

In Fig 10, velocity profiles from both the 2 in. and 3 in. test are plotted against time/scale factor (scale factor= 2 for the 2 in. test and 3 for the 3 in. test) in the usual geometric scaling fashion<sup>17</sup>. In the scaled time co-ordinate, we note that the wall velocity history for the 2-in. test is similar to the wall velocity history recorded in the 3-in. test for probes located nearer to the booster end of the 3 in. cylinder. This indicates that during the early evolution of the 3-in. test, the energy driving the wall expansion is similar in magnitude to the energy driving the wall in the 2-in. test in its quasi-steady propagation phase. However, as the detonation propagates further along the cylinder in the 3-in. test, the wall begins to expand faster relative to the geometrically scaled time as more energy is being delivered to the wall, presumably, as noted above, through additional late-time reaction of aluminum in the 3-in. test.

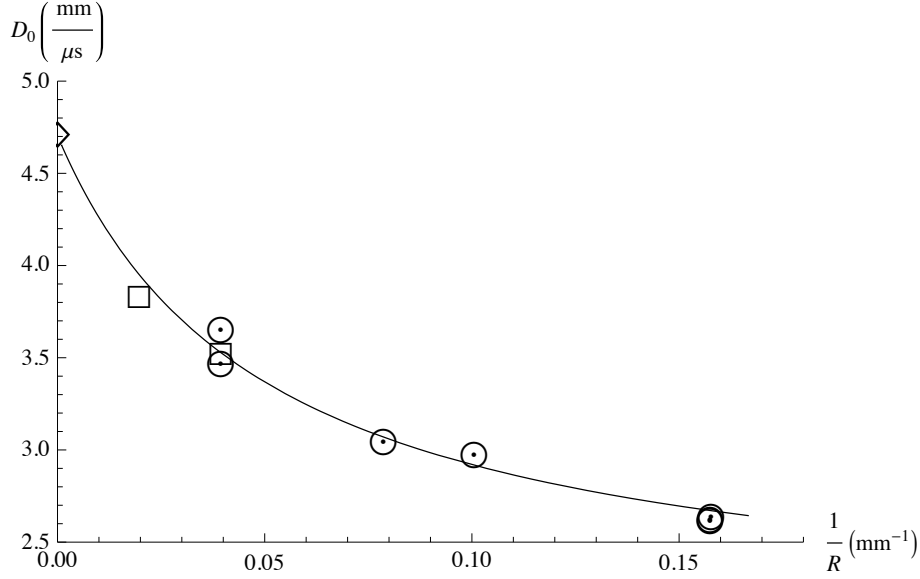


Fig. 2. Diameter effect for copper or steel confined cylindrical ammonal tests, blended at 90% ammonium nitrate, 10% aluminum. Results of the current study are indicated by the  $\square$  symbols, and results from previous experiments at LLNL<sup>12</sup> are indicated by the  $\odot$  symbols. The  $\diamond$  symbol indicates the CJ velocity for this blend computed with Cheetah<sup>15</sup>, and the curve represents a fit to the short Eyring form,  $D_0 = D_{CJ} \left(1 - \frac{A}{R-R_c}\right)$ , as described in Jackson and Short<sup>16</sup>.

#### Wall Velocity Measurements

Wall velocities are typically reported at standard scaled outer wall displacements of 6, 12.5, and 19 mm to allow comparison between different-sized cylinders. Since these displacements are scaled to a 1 in. ID cylinder test, they become 12, 25, and 38 mm for the 2 in. ID test, and 18, 37.5, and 57 mm for the 3 in. ID test.

In Table 4, radial wall velocities,  $v_r$ , for each PDV probe are reported at the three scaled outer wall displacements. Using these velocities, Gurney energy, a frequently-used measure of explosive product energy, can be computed with the equation:

$$G = \frac{1}{2} v_r^2 \left( \frac{1}{2} + \frac{m_w}{m_{HE}} \right), \quad (1)$$

where  $m_w$  is the wall mass per unit length, and  $m_{HE}$  is the explosive mass per unit length<sup>18</sup>. As stated in the equation, Gurney energy is the square of wall velocity multiplied by a factor that is constant for each cylinder test. This multiplier is 2.275 for the 2 in. ID test and 2.307 for the 3 in. ID test.

The slight discrepancy is due to the higher ammonal density for the 2 in. test. Gurney energy is typically reported at a scaled displacement of 19 mm as  $G_{19}$ . For the 2 in. ID test,  $G_{19}$  varies from 1.65 to 1.77 kJ/g, while that of the 3 in. ID test varies from 1.59 to 1.97 kJ/g.

The results of Table 4 show a great deal of consistency amongst the PDV probes for the 2 in. ID cylinder, with the exception of probe #8. The velocities measured by this probe are slightly lower, suggesting that the detonation is not yet fully developed at this axial ( $z$ ) location.

For the 3 in. ID cylinder, data was not acquired for probes #1 and #2. Probes #7 and #8 recorded lower velocities at each location compared to the other probes on this cylinder, indicating that the detonation is not yet steady at these locations. Probes #3–#6 recorded higher velocities for the 3 in. test than for the 2 in. test, indicating that 3 in. test is able to capture late aluminum reaction that is missed in the 2 in. cylinder test. All probes indicated that the velocity continues to increase past the 19 mm scaled

Table 4. Velocities extracted at scaled outer wall displacements.

Test ID	Probe #	PDV Velocity at Scaled Displacements		
		6 mm (mm/ $\mu$ s)	12.5 mm (mm/ $\mu$ s)	19 mm (mm/ $\mu$ s)
2	1	0.708	0.811	0.852
2	2	0.711	0.810	0.853
2	3	0.708	0.812	0.873
2	4	0.703	0.811	0.869
2	5	0.713	0.827	0.875
2	6	0.702	0.812	0.869
2	7	0.709	0.823	0.881
2	8	0.684	0.795	0.851
3	3	0.720	0.823	0.879
3	4	0.750	0.863	0.912
3	5	0.726	0.834	0.883
3	6	0.763	0.872	0.925
3	7	0.713	0.809	0.857
3	8	0.691	0.788	0.831

wall displacement, suggesting that aluminum reaction continues past this point in the cylinder expansion.

The results of 90% AN/10% Al cylinder tests reported by Souers et al.<sup>12</sup> are summarized in Table 5. While the aluminum and ammonium nitrate particle sizes were different, making direct comparison with the current effort difficult, a similar trend of increasing wall velocities with increasing cylinder diameter can be seen. The two tests conducted using 6.35 mm ID cylinders displayed substantially lower wall velocities than the 12.72 mm ID cylinder test, suggesting more energy from aluminum reaction is captured as the test is scaled up from 1/2 in. ID to 1 in. ID as well.

### Conclusions

Cylinder tests were performed using ammonal blended with 90 %AN/10% Al, extending the diameter of reported cylinder tests with this blend to 3 in. ID. Phase velocities were measured and found to be in good agreement with the Eyring form diameter-effect fit to previous metal-confined ammonal tests using the 90%/10% ratio. Successful PDV wall velocity measurements were obtained at eight loca-

tions for the 2 in. ID cylinder test and six locations for the 3 in. ID cylinder test.

For the 3 in. cylinder test, PDV profiles indicated that the detonation was not steady until beyond the probe located 1/3 of the way down length of the tube, whereas the detonation appeared quasi-steady at this location for the 2 in. test. Also, beyond the first 1/3 of the tube, the 3 in. test produced higher wall velocities than the 2 in. test. Both of these results suggest that aluminum releases more energy in the higher-temperature post-detonation expansion of the 3 in. test.

PDV measurements were used to compute the wall velocities at “standard” wall displacements, and as seen in the PDV profiles, more of the tube length was required to reach steady state for the 3 in. test. Also, higher velocities were recorded at each scaled wall displacement for the 3 in. test compared to the 2 in. test after the first 1/3 of tube length. Similar results were observed by Souers et al.<sup>12</sup> as tube diameters were increased from 0.5 in. to 1 in. using a 90 %AN/10% Al with different particle sizes.

Table 5. Results of 90% An/10% Al cylinder tests reported by Souers et al.<sup>12</sup>.

Density g/cm <sup>3</sup>	Al dia. μm	Det. Velocity mm/μs	Cyl. ID mm	Cyl. Wall mm	Vel. at Scaled Displacements		
					6 mm/μs	12.5 mm/μs	19 mm/μs
1.023	20	3.068	12.72	2.58	0.614	0.724	0.782
1.023	20	2.644	6.35	1.36	0.516	0.595	0.642
1.023	20	2.644	6.35	1.36	0.509	0.601	0.658

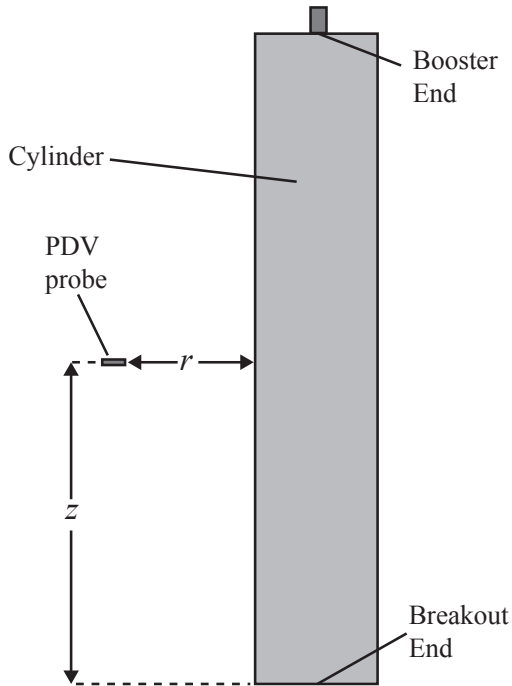


Fig. 3. Distances  $z$  and  $r$  which define the position of each PDV probe in Tables 2 and 3.

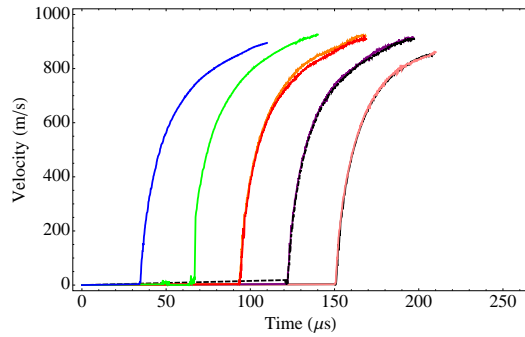


Fig. 4. Velocity profiles obtained for the 2 in. diameter cylindrical specimen.

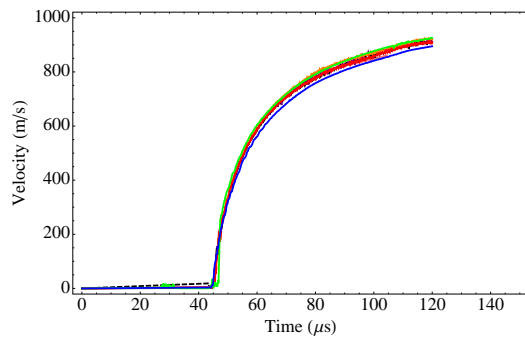


Fig. 5. Velocity profiles shifted along the x-axis for the 2 in. diameter cylindrical specimen.

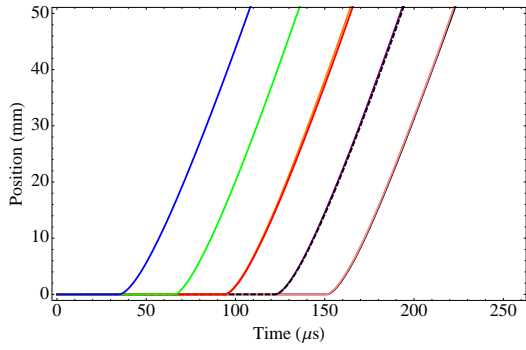


Fig. 6. Wall position profiles obtained for the 2 in. ammonal cylinder.

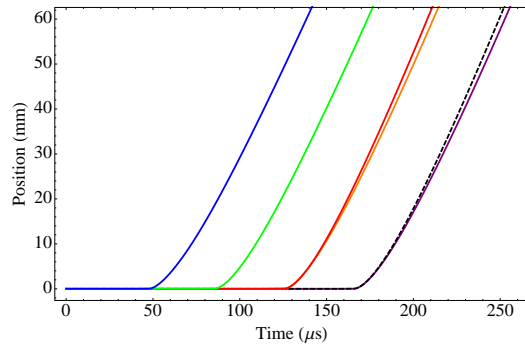


Fig. 9. Wall position profiles obtained for the 3 in. ammonal cylinder.

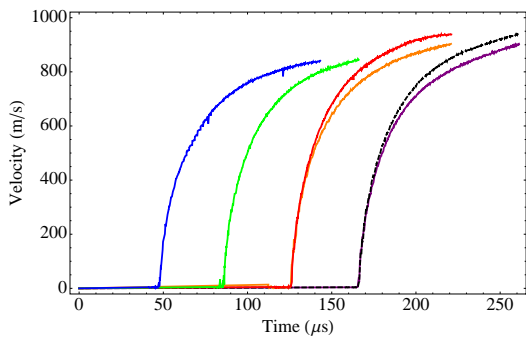


Fig. 7. Velocity profiles obtained for the 3 in. ammonal cylinder.

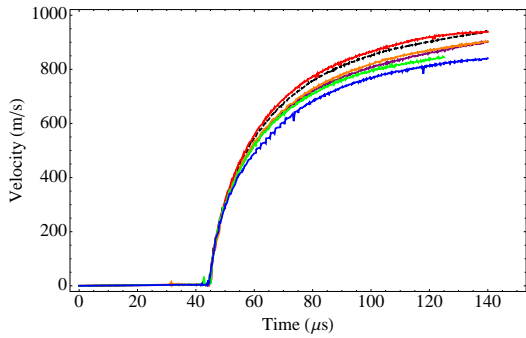


Fig. 8. Velocity profiles shifted along the x-axis for the 3 in. ammonal cylinder.

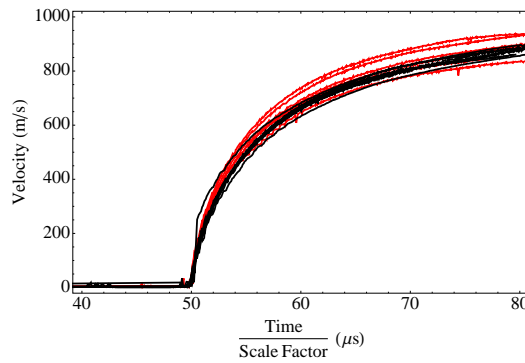


Fig. 10. Wall position profiles obtained for the 2 in. test (black) and the 3 in. test (red). Profiles are shifted along the x-axis to begin expansion at the same time, and the x-axis is also scaled by cylinder diameter.



## Acknowledgments

This effort was funded by the U.S. Department of Energy. The authors acknowledge Sam Vincent, Tim Kuiper, and Tim Pierce for their assistance with test assembly and fielding, Bryce Tappan and Pat Bowden their for assistance with ammonal preparation, and Kester Clarke for his expertise in metal conditioning. The authors would also like to to acknowledge Don Gilbert for grinding the ammonal components.

## References

1. Cook, M. A., Mayfield, E. B. and Partridge, W. S., "Reaction Rates of Ammonium Nitrate in Detonation," *The Journal of Physical Chemistry*, Vol. 59, pp. 675–680, 1955.
2. Zygmunt, B., "Detonation Parameters of Mixtures Containing Ammonium Nitrate and Aluminum," *Central European Journal of Energetic Materials*, Vol. 6, pp. 57–66, 2009.
3. Kuzmin, V., Kozak, G. and Mikheev, D., "Detonability of Ammonium Nitrate and Mixtures on Its Base," *Central European Journal of Energetic Materials*, Vol. 7, p. 335, 2010.
4. Maranda, A., "Research on the Process of Detonation of Explosive Mixtures of the Oxidizer Fuel Type Containing Aluminum Powder," *Propellants, Explosives, Pyrotechnics*, Vol. 15, pp. 161–165, 1990.
5. Glassman, I., *Metal Combustion Processes*, Defense Technical Information Center, 1959.
6. Law, C. K., "A Simplified Theoretical Model for the Vapor-Phase Combustion of Metal Particles," *Combustion Science and Technology*, Vol. 7, pp. 197–212, 1973.
7. Zhang, F., Murray, S. B. and Gerrard, K. B., "Aluminum particles–air detonation at elevated pressures," *Shock Waves*, Vol. 15, pp. 313–324, 2006.
8. Paszula, J., Trzcinski, W. A. and Sprzateczak, K., "Detonation Performance of Aluminium-Ammonium Nitrate Explosives," *Central European Journal of Energetic Materials*, Vol. 5, pp. 3–11, 2008.
9. Maranda, A., Lipinska, K. and Lipinska, M., "Analysis of Double Base Propellant Influence on Detonation Process of Ammonals," *Central European Journal of Energetic Materials*, Vol. 7, pp. 145–159, 2010.
10. Zygmunt, B. and Buczkowski, D., "Agriculture Grade Ammonium Nitrate as the Basic Ingredient of Massive Explosive Charges," *Propellants, Explosives, Pyrotechnics*, Vol. 37, pp. 685–690, 2012.
11. Buczkowski, D. and Zygmunt, B., "Detonation Properties of Mixtures of Ammonium Nitrate Based Fertilizers and Fuels," *Central European Journal of Energetic Materials*, Vol. 8, pp. 99–106, 2011.
12. Souers, P. C., Vitello, P., Garza, R. and Hernandez, A., "The Energy Diameter Effect," in "Proceedings of the APS Topical Group on Shock Compression of Condensed Matter," Vol. 955, pp. 877–880, American Institute of Physics, 2007.
13. Brousseau, P., Dorsett, H. E., Cliff, M. D. and Anderson, C. J., "Detonation Properties of Explosives Containing Nanometric Aluminum Powder," in "Twelfth Symposium (Int.) on Detonation," pp. 11–21, Office of Naval Research, 2002.
14. Kury, J. W., Hornig, H. C., Lee, E. L., McDonnell, J. L., Ornellas, D. L., Finger, M., Strange, F. M. and Wilkins, M. L., "Metal Acceleration by Chemical Explosives," in "Fourth Symposium (Int.) on Detonation," pp. 3–13, Office of Naval Research, 1965.
15. Fried, L. and Souers, P., "Cheetah: A Next Generation Thermochemical Code," *Technical Report URCL-ID-117240*, Lawrence Livermore National Laboratory, 1994.
16. Jackson, S. I. and Short, M., "Experimental Measurement of the Scaling of the Diameter-

and Thickness-Effect Curves for Ideal, Insensitive, and Non-Ideal Explosives,” in “Journal of Physics: Conference Series,” Vol. 500, American Institute of Physics, 2014.

17. Lee, E., Hornig, H. and Kury, J., “Adiabatic Expansion of High Explosive Detonation Products,” *Technical report*, California Univ., Livermore. Lawrence Radiation Lab., 1968.
18. Catanach, R., Hill, L., Harry, H., Aragon, E. and Murk, D., “Cylinder Test Specification,” *Technical Report LA-13643-MS*, Los Alamos National Laboratory, 1999.